

# Widespread divergent transcription from bacterial and archaeal promoters is a consequence of DNA sequence symmetry

Warman, Emily; Forrest, David; Guest, Thomas; Haycocks, James; Wade, Joseph T.; Grainger, David

DOI:

[10.1038/s41564-021-00898-9](https://doi.org/10.1038/s41564-021-00898-9)

License:

None: All rights reserved

*Document Version*

Peer reviewed version

*Citation for published version (Harvard):*

Warman, E, Forrest, D, Guest, T, Haycocks, J, Wade, JT & Grainger, D 2021, 'Widespread divergent transcription from bacterial and archaeal promoters is a consequence of DNA sequence symmetry', *Nature Microbiology*, vol. 6, no. 6, pp. 746-756. <https://doi.org/10.1038/s41564-021-00898-9>

[Link to publication on Research at Birmingham portal](#)

## General rights

Unless a licence is specified above, all rights (including copyright and moral rights) in this document are retained by the authors and/or the copyright holders. The express permission of the copyright holder must be obtained for any use of this material other than for purposes permitted by law.

- Users may freely distribute the URL that is used to identify this publication.
- Users may download and/or print one copy of the publication from the University of Birmingham research portal for the purpose of private study or non-commercial research.
- User may use extracts from the document in line with the concept of 'fair dealing' under the Copyright, Designs and Patents Act 1988 (?)
- Users may not further distribute the material nor use it for the purposes of commercial gain.

Where a licence is displayed above, please note the terms and conditions of the licence govern your use of this document.

When citing, please reference the published version.

## Take down policy

While the University of Birmingham exercises care and attention in making items available there are rare occasions when an item has been uploaded in error or has been deemed to be commercially or otherwise sensitive.

If you believe that this is the case for this document, please contact [UBIRA@lists.bham.ac.uk](mailto:UBIRA@lists.bham.ac.uk) providing details and we will remove access to the work immediately and investigate.

March 4<sup>th</sup> 2021

# **Widespread divergent transcription from bacterial and archaeal promoters is a consequence of DNA sequence symmetry**

**Emily A. Warman<sup>1</sup>, David Forrest<sup>1</sup>, Thomas Guest<sup>1</sup>, James J.R.J. Haycocks<sup>1</sup>,  
Joseph T. Wade<sup>2,3</sup>, David C. Grainger<sup>1\*</sup>**

<sup>1</sup>Institute for Microbiology and Infection, School of Biosciences, University of Birmingham,  
Edgbaston, Birmingham, B15 2TT, UK

<sup>2</sup>Wadsworth Centre, New York State Department of Health, Albany, NY, 12208, USA

<sup>3</sup>Department of Biomedical Sciences, University at Albany, Albany, NY, 12201, USA

\*for correspondence, d.grainger@bham.ac.uk Tel: +44 (0)121 4145437

## 1 ABSTRACT

2 Transcription initiates at promoters, DNA regions recognised by a DNA-dependent RNA  
3 polymerase. We previously identified horizontally acquired *Escherichia coli* promoters where the  
4 direction of transcription was unclear. Here, we show that more than half of these promoters are  
5 bidirectional. Using genome-scale approaches, we demonstrate that 19% of all transcription start  
6 sites detected in *E. coli* are associated with a bidirectional promoter. Bidirectional promoters are  
7 similarly common in diverse bacteria and archaea and have inherent symmetry: specific bases  
8 required for transcription initiation are reciprocally co-located on opposite DNA strands.  
9 Bidirectional promoters enable co-regulation of divergent genes and are enriched in both  
10 intergenic and horizontally acquired regions. Divergent transcription is conserved among  
11 bacteria, archaea and eukaryotes, but the underlying mechanisms for bidirectionality are  
12 different.

## 14 INTRODUCTION

15 Promoters are sections of duplex DNA that interact with RNA polymerase (RNAP) to stimulate  
16 transcription initiation<sup>1</sup>. In most organisms, promoters consist of ordered core elements with distinct  
17 roles<sup>2,3</sup>. For instance, the bacterial -10 element (consensus 5'-TATAAT-3') is usually indispensable and  
18 interacts with the housekeeping RNAP  $\sigma^{70}$  subunit ( $\sigma^A$  in some bacteria). The second and sixth positions  
19 of -10 elements are most critical; non-template strand bases interact with  $\sigma^{70}$  to stabilise DNA  
20 unwinding<sup>4,5</sup>. Position one is also important, and defines the upstream boundary of DNA melting<sup>5</sup>. Less  
21 conserved ancillary sequences can aid RNAP recruitment. For instance, the -35 element (consensus  
22 5'-TTGACA-3') also contacts  $\sigma^{70}$ . Following initiation,  $\sigma^{70}$  is evicted from the elongation complex. In  
23 many eukaryotes and archaea, the TATA box functions analogously to the bacterial -10 element; TATA  
24 binding protein (TBP) facilitates DNA unwinding and serves as a scaffold for recruiting the  
25 transcriptional apparatus<sup>6</sup>.

27 It has long been assumed that promoter sequences are directional, driving transcription in a single  
28 orientation determined by promoter element arrangement<sup>2,7</sup>. This view has been challenged in  
29 eukaryotes<sup>8-11</sup>. In addition to driving the production of a canonical sense mRNA, many RNAP II  
30 promoters simultaneously stimulate antisense transcription<sup>12</sup>. Permissive chromatin plays a key role;  
31 nucleosome-depleted DNA allows fortuitous binding of transcriptional activators that permit divergent  
32 transcription<sup>12-15</sup>. Thus, permissive sections of eukaryotic chromatin, not core promoters *per se*, give  
33 rise to bidirectionality<sup>9,12,13,16</sup>. The phenomenon is particularly prevalent for recently evolved promoter  
34 regions suggesting that, if beneficial, selection can fix mutations that favour unidirectional  
35 transcription<sup>16</sup>. In prokaryotic organisms, particularly the bacteria, chromosomes are not folded into  
36 structures reminiscent of eukaryotic chromatin<sup>17</sup>. The consensus view remains that transcription from

bacterial promoter sequences is unidirectional<sup>18</sup>. Here, we show that bidirectional prokaryotic promoter sequences, resulting in divergent transcription, are in fact commonplace. However, the underlying molecular mechanisms are fundamentally different to those in eukaryotes.

## RESULTS

### *Identification of bidirectional promoter sequences in horizontally acquired Escherichia coli genes*

Transcription start sites (TSSs) in *Escherichia coli* have been mapped by detecting triphosphorylated RNA 5' ends<sup>19</sup>. These can be assigned to  $\sigma^{70}$  binding events identified using ChIP-seq<sup>19</sup>. We noticed that not all  $\sigma^{70}$  binding was associated with detectable RNA synthesis. This was particularly evident for horizontally acquired genes silenced by histone-like nucleoid structuring (H-NS) protein (Extended Data Fig. 1). We reasoned that RNAP might initiate transcription, but produce unstable RNAs, at these sites; similar to cryptic unannotated transcripts in eukaryotes<sup>12</sup>. To test this, we transcriptionally fused 33 such  $\sigma^{70}$  targets, derived from H-NS silenced genes, to *lacZ*. Translation prevents Rho mediated transcription termination. Hence, any RNAs produced should be stabilised and detectable<sup>20</sup>. As transcription orientation cannot be directly inferred from  $\sigma^{70}$  ChIP-seq data, DNA sequences were cloned in both directions (Fig. 1a). Over half of the fragments were transcriptionally active ( $\geq 2$ -fold above the background control) regardless of orientation (Fig. 1b). We designated the direction of highest *lacZ* expression as “forward”. On average, “reverse” transcription neared half the “forward” activity (Fig. 1c). We repeated the experiment with 25 well-characterised promoter DNA fragments<sup>21</sup>. Importantly, we selected only promoters that did not contain a detectable TSS on the opposite DNA strand<sup>19,22,23</sup>. Such DNA fragments could only drive *lacZ* expression in the “forward” orientation (Extended Data Fig. 2). For an arbitrary subset of TSS pairs, we mapped RNA 5' ends (Fig. 1d). This allowed annotation of promoter elements (Fig. 1e). For the *yibA2* DNA fragment, TSSs were convergent. For all other DNA fragments, TSSs were divergent. Hence, promoter elements for oppositely oriented transcripts mapped, partially or completely, to the same section of DNA (Fig. 1e and Extended Data Fig. 3). Mutation of these shared promoter sequences (Fig. 1e and Extended Data Fig. 3) reduced expression in both orientations (Fig. 1f).

### *Bidirectional promoter sequences are widespread and obey precise organisational rules*

To understand global patterns of divergent transcription we analysed TSSs mapped by RNA 5' polyphosphatase sequencing (PPP-seq), dRNA-seq or cappable-seq<sup>19,22,23</sup>. Oppositely orientated TSSs tended to co-locate (Fig. 2a). To increase sensitivity, we merged the datasets (Fig. 2a, combined). This identified 5,292 divergent TSSs, defined as being separated by between 25 and 7 bp; 19 % of all detected TSSs in *E. coli* (Table S1). We refer to the associated promoter sequences as “bidirectional” and the corresponding TSSs as “divergent TSS pairs”. The most common distance between divergent TSS pairs was 18 bp (Fig. 2a, top expansion). This corresponds to transcription initiation, on opposite

DNA strands, either side of the same promoter -10 region (Fig. 2a, top expansion). Presumably, promoter element symmetry must play a major role in creating bidirectional promoter sequences. To test this, we made a position weight matrix (PWM) describing all *E. coli* promoter sequences. The PWM was aligned with its reverse complement across a range of spacings (i.e. altered stagger between forwards and reverse PWM). We then calculated a symmetry score for each spacing. If the PWM resembled the same section of DNA in both orientations, the symmetry score increased. There was strong correlation between experimentally detected divergent TSS pairs and those predicted on the basis of symmetry score ( $R^2 = 0.85$ ; Fig. 2a bottom expansion). Consistent with this, a DNA sequence logo generated by aligning divergent TSSs, separated by 18 bp, was symmetrical (Fig. 2b). Contrastingly, TSSs with no divergent transcript generated an asymmetrical motif (Fig. 2c). Recall that the second and sixth positions of  $\sigma^{70}$  promoter -10 elements are crucial<sup>5</sup>. Non-template strand bases at these positions, relative to the orientation of RNAP binding, are sequestered by  $\sigma^{70}$  to stabilise initial duplex melting<sup>5</sup>. At divergent TSS pairs offset by 18 bp, these key bases reciprocally coincide on opposite DNA strands. Hence, these positions are strongly conserved (Fig. 2b). An example of a -10 element with such symmetry is shown in Fig. 2d; the critical bases at positions two and six are underlined. Divergent transcription was also enriched for TSS pairs offset by 23, 12, 10 or 7 bp (Extended Data Fig. 4a). These configurations also correspond to reciprocal base pairing between key -10 element nucleotides and TSSs (Extended Data Fig. 4b). We note that, of the divergent TSS pairs detected within horizontally acquired sequences, two match one of the common configurations (Fig. 1). For instance, the divergent TSSs within *yigG* are 7 bp apart. To test whether the symmetrical sequences were intrinsically able to drive divergent transcription we used *in vitro* transcription assays. Bidirectional promoter sequences were cloned, in either the forward or reverse orientation, upstream of the  $\lambda$ oop terminator in plasmid pSR. Transcripts terminated by  $\lambda$ oop have a defined length and can be detected using electrophoresis. In all cases, regardless of the cloning orientation, bidirectional promoter sequences produced detectable transcripts terminated by  $\lambda$ oop (Extended Data Fig. 4c,d). Since *in vitro* transcription assays use no protein factors other than RNAP, divergent transcription must be an intrinsic property of bidirectional promoter DNA sequences.

#### *Molecular basis for promoter sequence bidirectionality: a dual role for transcription start sites*

In *E. coli* transcription preferentially initiates at an adenine (Fig. 2c). For divergent TSSs 18 bp apart, the +1 nucleotide corresponds to position -18 on the opposite DNA strand. Hence, -18 is most often a thymine (Fig. 2b). A thymine at position -18 can increase transcription by altering DNA bending<sup>24</sup>. This change in DNA conformation enhances the interaction between the nearby  $\sigma^{70}$  residue R451 and the DNA backbone<sup>24</sup> (Fig. 3a). Importantly, this can negate the need for a -35 element<sup>25</sup>. We speculated that the +1/-18 overlap could explain why this configuration is most frequently detected. To test this, we cloned a bidirectional promoter sequence, with 18 bp between TSSs, in both orientations upstream

of the *loop* transcriptional terminator (Fig. 3bi). We also made derivatives where the A•T at each +1/-18 position was replaced with C•G (Fig. 3bii-iii). Note that cloning in both orientations was necessary because transcription directed away from *loop* is not precisely terminated. Hence, a discrete transcript is not produced. As expected, altering the TSS reduced production of the associated RNA (Fig. 3c, compare lane 1 with 5 and 3 with 11); the same mutations also reduced transcription in the opposite direction (compare lane 1 with 9 and 3 with 7). Though  $\sigma^{70}$  RA451 was defective at the bidirectional promoter sequences (even lane numbers to 12) it was unimpaired at a control promoter not requiring this contact (lanes 13-14).

#### *Bidirectional promoter sequences are overrepresented at sites of mRNA synthesis*

Of all divergent TSS pairs, 48% located to intergenic DNA (Fig. 2e). Of the resulting transcripts, 75 % are expected to be mRNAs, based on the orientation of the flanking genes. By comparison, only 29 % of directional TSSs were in intergenic regions, near a gene 5' end, with 89 % of associated transcripts expected to be mRNAs (Extended Data Fig. 5d). This suggests many bidirectional promoter sequences control gene expression. Hence, we determined if divergent TSS pairs mapped to well-characterised promoters, known to control mRNA production, listed in RegulonDB<sup>26</sup>. First, we examined the RegulonDB set of 317 mRNA TSSs identified by 5' RACE<sup>27</sup>. Of these TSSs, 311 were in our combined TSS dataset; a 156-fold enrichment compared to random genome co-ordinates. Enrichment was significantly more pronounced for divergent TSS pairs (252-fold) than directional TSSs (136-fold) ( $P = 0.002$ , Fisher's exact test). RegulonDB lists a further 3,330 mRNA TSSs, identified using numerous approaches, according to RNAP  $\sigma$  factor specificity<sup>26</sup>. The majority are  $\sigma^{70}$  dependent<sup>26</sup>. Of the 1,994  $\sigma^{70}$  dependent TSSs, 1,410 are in our combined TSS dataset (a 113-fold enrichment). Moreover,  $\sigma^{70}$  dependent TSSs are significantly overrepresented amongst divergent TSS pairs (133-fold enrichment) compared to directional TSSs (108-fold enrichment) ( $P = 0.032$ , Fisher's exact test). Conversely, RegulonDB described promoters for alternative  $\sigma$  factors do not preferentially map to divergent TSS pairs (Table S2). This is consistent with divergent TSS pairs mapping to sequences resembling the  $\sigma^{70}$  -10 element (Fig. 2b and Extended Data Fig. 4b).

#### *Length and stability of transcripts arising from bidirectional promoter sequences*

To investigate length and stability of transcripts from bidirectional promoter sequences we used RNA-seq. We focused on divergent TSS pairs in non-coding regions; overlapping mRNA synthesis confounds analysis of intragenic promoters. After grouping intergenic loci according to adjacent gene orientation, we generated aggregate RNA coverage plots (Fig. 3d and 3e). At bidirectional promoter sequences between co-oriented genes, RNAs generated in each direction had different properties (Fig. 3d). Whilst non-coding antisense transcripts were detectable, coding transcripts were more abundant and longer. For bidirectional promoter sequences between divergent genes, two coding RNAs are expected. Hence,

transcript abundance and length was similar in both directions (Fig. 3e). Fig. 3f illustrates examples of RNAs derived from divergent TSS pairs. Note that cappable-seq detects only RNA 5' ends whilst RNA-seq detects all RNA sequences.

#### *Bidirectional promoter sequences are widespread in bacteria*

Widespread divergent transcription from bacterial promoters has not been reported previously. However, a prior study did identify a modest number of divergent TSS pairs offset by 18 bp in *Pseudomonas aeruginosa*<sup>28</sup>. To determine the prevalence of bidirectional promoter sequences across the bacterial kingdom we analysed TSS maps for proteobacteria<sup>19,22,23,28–31</sup>, actinobacteria<sup>32,33</sup>, and a firmicute<sup>34</sup>. We also mapped TSSs in an additional firmicute, *Bacillus subtilis*, using cappable-seq (Extended Data Fig. 5 and Table S3). Co-localised divergent TSSs were abundant in all bacteria analysed (Fig. 4a). Proteobacteria and actinobacteria were most similar; divergent TSS pairs were usually offset by 18 or 19 bp as in *E. coli* (Extended Data Fig. 6). Firmicutes used the same range of -10 element configurations illustrated in Extended Data Fig. 4 for *E. coli* but with little preference for a single arrangement (Extended Data Fig. 6).

#### *Bidirectional promoter sequences in archaea and bacteria are analogous*

Archaeal transcription is closely related to that of eukaryotes; promoters have a TATA box and B recognition element (BRE; 5'-CGAAA-3'), located a narrow range of distances from the TSS<sup>35</sup>. Previously, Grünberger and co-workers noted divergent transcription from sites either side of a shared TATA box in *Pyrococcus furiosus*<sup>36</sup>. This resembles the scenario presented here for bacteria. We speculated that bidirectional promoter sequences should be widespread in archaea with multiple spacing preferences evident. We analysed TSS maps for the archaea *Thermococcus kodakarensis* and *Haloferax volcanii*<sup>37,38</sup>. We observed strong signatures of promoter sequence bidirectionality (Fig. 4a). In *T. kodakarensis*, divergent TSS pairs were predominantly offset by 52 bp, and located either side of a shared TATA box element (5'-TTATAAA-3') (Fig. 4b,c and Extended Data Fig. 7a). Less frequently, divergent TSS pairs were offset by 36 bp (Fig. 4b and Extended Data Fig. 7a). In this situation, the BRE is positioned so the initial C•G bp can also act as the TSS on the opposite DNA strand (Fig. 4c). Similar observations were made for *H. volcanii* despite the unusual TATA box consensus (5'-TTWT-3') of haloarchaea (Extended Data Fig. 7b,c).

#### *Promoter sequences acquired by horizontal gene transfer are more frequently bidirectional*

In eukaryotes, bidirectional promoters occur more frequently in recently acquired DNA<sup>16</sup>. We have shown that horizontally acquired bacterial genes, by virtue of their high AT-content, are enriched for promoter -10 elements and TSSs<sup>19,39</sup>. We reasoned that many such sites could represent bidirectional promoter sequences. Indeed, our initial analysis of 33  $\sigma^{70}$  binding events, within horizontally acquired

DNA, is consistent with this view (Fig. 1). As predicted, detection of divergent TSS pairs using PPP-seq, increased in cells lacking H-NS; a protein that suppresses transcription at horizontally acquired DNA (Extended Data Fig. 8a). Parallel DNA sequence analysis demonstrated elevated promoter symmetry in foreign genes (Extended Data Fig. 8b). To understand other bacteria we utilised the TSS datasets described above. For both directional and bidirectional promoter sequences we determined the percentage of associated TSSs mapping to horizontally acquired sections of the cognate genome. Bidirectional promoter sequences were enriched in horizontally acquired regions for 6 of the 8 genomes analysed (Extended Data Fig. 8c).

#### *Bidirectional promoter sequences allow coordinated regulation of divergent operons*

The widespread occurrence of bidirectional promoter sequences has implications for our understanding of gene regulation. In the bacterium *Vibrio cholerae*, the genes VC1303 and VC1304 encode a para-aminobenzoate synthetase and a fumarate hydratase respectively. The divergent coding sequences share the same gene regulatory region (Fig. 5a). Examination reveals a divergent transcription start site pair with 23 bp spacing; the second most common configuration in both *E. coli* and *V. cholerae* (Fig. 5a and Extended Data Fig. 4). Here, reciprocal base pairing is observed between -10 element positions one and two (underlined in Fig. 5a). The intergenic region is also a target for the cyclic-di-GMP responsive transcription factor VpsT (identified using ChIP-seq, data to be presented elsewhere). Binding of VpsT was confirmed using DNaseI footprinting. As expected, in the absence of cyclic-di-GMP, VpsT was unable to bind the regulatory DNA (Fig. 5b, lanes 1-5). Conversely, in the presence of cyclic-di-GMP, VpsT protected a ~50 bp section of DNA from digestion (Fig. 5b, lanes 6-10). The expansion in Fig. 5a illustrates that the VpsT footprint overlaps the bidirectional -10 element. To investigate the impact of VpsT on transcription in each orientation, we first used *in vitro* transcription assays. We cloned the regulatory DNA, in either orientation, upstream of the *loop* terminator in plasmid pSR. In the absence of VpsT, transcripts of the expected size were detected in each orientation (Fig. 5c, lanes 1 and 3). When VpsT was added, production of both transcripts was greatly reduced (Fig. 5c, lanes 2 and 4). To understand the effect of VpsT *in vivo* we cloned the same promoter DNA fragment, in either orientation, upstream of *lacZ* in plasmid pRW50T. In both orientations, promoter activity was significantly reduced in *V. cholerae* expressing VpsT (Fig. 5d).

#### *RNA polymerase complexes compete at bidirectional promoter sequences*

At bidirectional promoter sequences RNAP can bind the same section of duplex DNA in two possible orientations. This binding cannot be simultaneous; structural constraints preclude this<sup>40</sup>. Instead, RNAP molecules likely compete to access the DNA duplex. We hypothesised that increased RNAP binding in one orientation would reduce transcription in the opposite direction. Since the promoter -35 element stabilises RNAP binding we introduced this sequence either side of a bidirectional -10 region. Our initial attempts to clone such DNA fragments in plasmid pSR failed. Specifically, we could not isolate



recombinants with DNA inserts expected to generate high levels of reverse transcription. We reasoned that such transcription might interfere with expression of the upstream *bla* gene. Hence, we utilised a derivative of pSR with a *loop* terminator positioned upstream, as well as downstream, of the cloned DNA. The DNA constructs generated are shown in Fig. 5e. The presence of two transcriptional terminators allowed simultaneous detection of both forward and reverse RNA products following *in vitro* transcription (Fig. 5f, lane 1) dependent on  $\sigma^{70}$  side chain R451 (lane 2). Addition of a -35 element upstream of the -10 sequence increased transcription in the forward direction (lane 3, lower band). Concurrently, transcription in the reverse direction was reduced (lane 3, upper band). The inverse result was obtained if the -35 element was introduced downstream of the -10 region (compare lanes 3 and 5). When both -35 elements were present levels of divergent transcription increased in both directions (lane 7). However, increases were smaller than those detected with individual -35 elements (compare lanes 3, 5 and 7). Note that promoter -35 elements removed the requirement for  $\sigma^{70}$  residue R451 (compare lane 2 with lanes 4, 6 and 8). Indeed, the  $\sigma^{70}$  R451A derivative was moderately more active in such instances. Most likely, the R451-DNA contact hinders escape from near consensus promoters.

## DISCUSSION

We demonstrate that divergent transcription from promoter sequences is a process conserved in all domains of life. The phenomenon is similarly frequent in diverse prokaryotes (Extended Data Fig. 9) and superficially resembles the situation in eukaryotes. However, the mechanistic basis is fundamentally different (Fig. 6). In eukaryotes, chromosomal regions associated with divergent transcription are large; bidirectionality is generated by nucleosome-depleted DNA and fortuitous binding of transcriptional activators<sup>12–15</sup>. Hence, divergent transcripts initiate from easily distinguishable sites separated by hundreds or thousands of base pairs, with no distance optimal. Accordingly, each TSS is associated with a distinct RNAP binding event involving non-overlapping DNA regions<sup>9,12,13,16</sup>. By contrast, bidirectional promoter sequences in bacteria have inherent symmetry. Hence, RNAP can bind the same section of duplex DNA in either orientation. Our global TSS analysis shows that symmetrical -10 elements are the main driver of divergent transcription (Fig. 2). This is consistent with the unique role of this promoter motif. Thus, whilst other promoter sequences stabilise RNAP binding, the -10 element also facilitates DNA opening and transcription initiation. Accordingly, ancillary promoter sequences are ineffective without an appropriately positioned -10 motif. We show that -10 elements, with inherent symmetry, can function independently to drive divergent transcription (Fig. 3c and Extended Data Fig. 4c). In the most common situation, the +1 and -18 positions on opposite strands align. This enhances the ability  $\sigma^{70}$  side chain R451 to stabilise RNAP binding. Interestingly, one example of a bidirectional -35 element was identified within the horizontally acquired *ygaQ* gene (Fig. 1e). We speculate that such configurations are more likely to arise in foreign DNA; the high AT-content ensures many potential -10 sequences are available. As in bacteria, divergent TSS pairs in

archaea are separated by preferred distances, corresponding to key bases for transcription initiation overlapping on opposite DNA strands (Fig. 4c and Extended Data Fig. 7). The separation of TSSs by 34 bp and 36 bp in *H. volcanii* and *T. kodakarensis* respectively corresponds to alignment of the BRE (important for RNAP binding) and the +1 site of initiation on the opposite DNA strand. This is similar to alignment of positions -18 and +1 in bacteria.

Remarkably, despite the differences between prokaryotes and eukaryotes, our data suggest divergent transcription is often a property of newly acquired DNA in both kingdoms. Thus, nascent promoters can be inherently bidirectional. In bacteria, this is likely a consequence of both the DNA motif for divergent transcription, and horizontally acquired loci, having a high AT-content<sup>19</sup>. The abundance of non-canonical promoter elements is also likely to play a role<sup>41</sup>. Most sites of transcription within horizontally acquired genes are associated with non-coding RNA production. However, bidirectional promoter sequences elsewhere drive mRNA synthesis. Indeed, compared to directional promoters, divergent TSS pairs are more frequently found in intergenic regions, particularly between divergent genes (Fig. 2e and Extended Data Fig. 5d). Hence, divergent transcription must also have important implications for gene expression. For instance, we show that transcriptional repressors can co-regulate divergent operons by binding sites that overlap a bidirectional promoter sequence (Fig. 6). We also show that frequency of transcription in a given orientation impacts divergent RNA synthesis (Fig. 5f). Hence, bidirectional promoter sequences have inbuilt regulatory properties. Speculatively, divergent transcription could also displace adjacently bound transcription factors or generate asRNAs impacting adjacent genes. In conclusion, the widespread occurrence of bidirectional promoter sequences has important implications for understanding gene regulation in all prokaryotes.

## MATERIALS AND METHODS

### *Strains, plasmids and oligonucleotides*

All strains plasmids and oligonucleotides used are listed in Table S4. Standard procedures for strain and DNA manipulation were used throughout. All bacterial cultures were grown in LB media.

### *β-galactosidase assays*

Assays were done according to the method of Miller<sup>42</sup>. Cells were grown in LB media supplemented with appropriate antibiotics to mid-log phase. Values shown are the mean of three independent experiments. Error bars represent the standard deviation of three independent experiments. Promoters were characterised as active if they stimulated β-galactosidase activity >2-fold over background levels generated by promoterless *lacZ*.

### *Identification of transcription start sites by primer extension*

Transcript start sites were mapped for individual promoters using primer extension as described by Haycocks and Grainger<sup>43</sup>. The RNA was purified from indicated *E. coli* strains carrying different DNA fragments cloned in pRW50. The 5' end-labelled primer D49724, which anneals downstream of the *HindIII* site in pRW50, was used in all experiments. Primer extension products were analysed on denaturing 6% polyacrylamide gels, calibrated with size standards, and visualized using a Fuji phosphor screen and Bio-Rad Molecular Imager FX.

#### *Genome-wide identification of divergent transcription start site pairs*

Divergent TSS pairs at bidirectional promoter sequences were identified by calculating the distance between each TSS on the top and bottom DNA strands. The TSS were classified as divergent pairs if the bottom strand TSS was between 7 and 25 bp upstream of the top strand TSS. If a TSS on a given DNA strand could couple with multiple TSSs on the opposite DNA strand these were each counted as separate TSS pairs. Similarly, if directional promoter sequences were associated with multiple TSSs these also were individually counted. To compare TSSs in wild type *E. coli*, and the  $\Delta hns$  derivative, we used our previously generated data<sup>19</sup> and remapped TSSs. This was done using TSSpredator (version 1.06)<sup>44</sup> with the following settings: step height 0.1, step height reduction 0.09, step factor 1.5, step factor reduction 0.5, enrichment factor 3, normalisation percentile 0.9, enrichment normalisation percentile 0.5, UTR length 300 and antisense UTR length 100. Cluster method was set to HIGHEST and all other parameters were set to 0. For all other datasets, we used TSS locations provided by the original studies. We designated TSSs as likely to drive mRNA synthesis if they were intergenic and in the correct orientation upstream of a gene. Note that previous PPP-seq analysis<sup>19</sup> was done according to the protocol of Singh and Wade<sup>45</sup>.

#### *Promoter symmetry scoring*

To determine symmetry scores, we derived a PWM corresponding to sequences from -100 to +50 bp relative to each TSSs for each species test. We refer to this as the “forward PWM”. (Note that for the heatmap in Fig. 2a, the forward PWM was derived from sequences from -100 to +100 to facilitate analysis over a longer range of spacings; importantly, this does not impact the calculated scores). We then made a “reverse PWM” that corresponds to the reverse complement of the forward PWM, but was limited to sequences from -37 to +5 relative to the TSSs, since this is the range that includes all key promoter elements for all species tested. We aligned the forward and reverse PWMs across all possible spacing combinations. For each spacing, we calculated a symmetry score by (i) multiplying the fraction of each of the four nucleotides at each position of the forward PWM with the fraction of each of the complementary nucleotides at the overlapping position of the reverse PWM, and (ii) multiplying this value by 4, taking the log (base 2), and summing for all positions within the overlapping PWM positions. Stated  $R^2$  values are Pearson product-moment correlation coefficients generated by comparing symmetry scores with TSS spacing abundance across the spacing range shown. Symmetry

scores were also calculated for individual *E. coli* promoter sequences, to compare promoter sequences in horizontally acquired versus non-horizontally acquired regions, and to compare promoter sequences in H-NS-bound versus unbound regions. In these cases, we analysed individual promoter regions from position -100 to +50 relative to the TSS. We aligned the reverse PWM for *E. coli* (derived as described above) with each promoter sequence across all possible spacings. For each spacing, we determined the frequency of the nucleotide found in the promoter with the corresponding nucleotide frequency in the reverse PWM. We then multiplied these values for every position within the PWM. The final symmetry score for each promoter sequence was calculated as the maximum score across all possible spacings multiplied by a constant (to avoid extremely small numbers).

#### *Promoter sequence analysis*

To determine the distance between TSSs and promoter -10 elements we searched for the sequence 5'-TANNNT-3' in the 17 bp region upstream of the TSS. If this sequence did not occur, or occurred multiple times, the TSS was excluded to avoid ambiguities. To generate DNA sequence motifs we used Weblogo<sup>46</sup>. For directional *E. coli* promoters we created two alignments, anchored by either the position of the TSS or -10 element, that were then spliced together in the intervening DNA. This was required because the spacing between the +1 and -10 entities is variable (Extended Data Fig. 5a) and results in improper alignment unless taken into account (compare Fig. 2c and Extended Data Fig. 5b). This adjustment was not required for bidirectional promoters with TSSs separated by 18 bp (Fig. 2b). In this situation, juxtaposition of the TSSs and -10 elements are “locked” in place in accordance with Fig. 3 and the associated description.

#### *Proteins*

The *V. cholerae* RNAP holoenzyme was purified as described previously<sup>47</sup>. To facilitate overexpression, *vpsT* was cloned in pET28a and the resulting construct used to transform T7 express cells. Resulting transformants were used to inoculate 20 ml of LB media that was incubated overnight with shaking at 37 °C. Subsequently, this culture was used to inoculate 2 L of fresh LB media. The resulting culture was incubating at 37 °C with shaking until the OD<sub>650</sub> reached 0.8. Overexpression of the encoded His<sub>6</sub>-VpsT fusing was induced with 1 mM IPTG for 16 hours at 18 °C. Cells were then recovered by centrifugation, resuspended in 25 mM Tris-HCl pH 7.5, 550 mM NaCl, 20 mM Imidazole, and lysed by sonication. The cleared lysate was applied to a HisTrap (Amersham) column and bound proteins eluted with an imidazole concentration gradient up to 500 mM. Fractions containing VpsT were pooled and transferred into 25 mM Tris-HCl pH 7.5, 100 mM NaCl, 5 % (v/v) glycerol by dialysis. Contaminating proteins were removed using a HiTrap heparin HP (Amersham) column and pure His<sub>6</sub>-VpsT was eluted with concentration gradient up to 1 M NaCl. Fractions containing the pure protein were pooled and concentrated to 1 mg/ml using a Vivaspin (Sartorius) concentrator. Precipitated protein was removed by filtration and the His<sub>6</sub> tag removed by thrombin digestion. The cleaved tag was

separated from VpsT in a final HisTrap chromatography step. The pure VpsT was concentrated to 1 mg/ml and glycerol added to a final concentration of 50 % (v/v) for storage.

#### *in vitro transcription assays*

*In vitro* transcription reactions used the method of Kolb *et al.*<sup>48</sup> as described by Savery *et al.*<sup>49</sup>. Plasmid template DNA was isolated from *E. coli* transformed with pSR containing the appropriate promoter DNA fragment. Reaction buffer contained 20 mM Tris pH 7.9, 200 mM GTP/ATP/CTP, 10 mM UTP, 5  $\mu$ Ci ( $\alpha^{32}$ P) UTP, 500 mM DTT, 5 mM MgCl<sub>2</sub>, 100  $\mu$ g ml<sup>-1</sup> BSA and 0.2 mM cAMP. Template DNA (at a final concentration of 16  $\mu$ g ml<sup>-1</sup>) was incubated with RNAP holoenzyme, derived from either *E. coli* or *V. cholerae* as appropriate, to start the reaction.

#### *Comparison with mRNA transcription start sites listed by RegulonDB*

Matches between the combined TSS list, and TSSs listed in RegulonDB, were identified using the COUNTIF function in Microsoft Excel. When matching TSSs in RegulonDB to the combined list of *E. coli* TSSs we allowed a +/- 2 bp leeway. This was done because positions of equivalent TSSs, identified using different methods, often vary slightly. Additionally, RNAP can initiate transcription from a single promoter at one of several adjacent nucleotides. To calculate fold enrichment we first determined how many known TSSs listed in RegulonDB matched TSSs in our combined dataset. We then determined how many matches were identified if the positions of TSSs in our combined dataset were randomised to any position in the genome. To calculate the stated fold enrichment the former result was divided by the latter. We used the same approach with subsets of the combined TSS dataset corresponding to directional or bidirectional promoter sequences. We note that, in all cases, similar results were obtained if the positions of TSSs in our combined dataset were instead randomised to equivalent genomic contexts (i.e. intragenic and intergenic promoters to coding and non-coding regions respectively). This was expected because 19 % of TSSs in the combined list were in intragenic regions. This is comparable to the 12 % of the *E. coli* genome annotated as non-coding. To test for significant enrichment of different TSSs groups in RegulonDB, amongst the combined list of TSSs presented here, we used a hypergeometric test. For this test, the number of successful draws was the number of RegulonDB TSSs identified amongst the set of divergent 5,292 TSSs or the set of 23,813 directional TSSs (i.e. the total number of draws). The population size was 4,639,675 (i.e. the number of bp in the *E. coli* U00096.2 genome) and the number of successes in the population was the number of TSSs in the RegulonDB group being tested. To determine if there was a significant difference between the number of RegulonDB TSSs found in the lists of divergent TSSs and directional TSSs we used Fisher's exact test. Our null hypothesis was no difference in enrichment. To determine the expected number of RegulonDB promoters amongst the bidirectional TSSs, we calculated the relative frequency of RegulonDB promoters in the set of 23,813 directional TSSs. We then multiplied the relative frequency value by 5,292 (the number of divergent TSSs). These values were then compared to the experimental data.

#### *Mapping global transcript abundance by RNA-seq*

Duplicate cultures of *E. coli* strain MG1655 were grown until mid-exponential phase in LB media with shaking at 37 °C. Cells were harvested by centrifugation, flash frozen in liquid nitrogen, and lysed by RNAsnap<sup>50</sup>. Total RNA was then purified from lysates using the Qiagen Mini RNeasy kit. Library preparation and sequencing was done by Vertis Biotechnologie AG. Briefly, RNA molecules were fragmented by sonication before ligation to oligonucleotide adapters at their 3' end. First-strand cDNA synthesis was done using M-MLV reverse transcriptase and the 3' adapter as primer. The first-strand cDNA was purified and the 5' Illumina TruSeq adapter was attached at the 3' end. After PCR amplification the cDNA was purified using the Agencourt AMPure XP kit (Beckman Coulter Genomics) and analysed by capillary electrophoresis. Libraries were sequenced on an Illumina Nextseq 500 system with a read length of 75 bp. Fastq files were deposited in Array Express (accession number E-MTAB-9655). Individual sequence reads were mapped using Bowtie2<sup>51</sup>. The reference genome for *E. coli* was that assigned Genbank accession number U00096.3. Resulting Binary Alignment Map (BAM) files were used to generate wiggle plots using bam2wig.py<sup>52,53</sup>. These data, were used to generate the aggregate plots shown in Fig. 3. For each dataset, we calculated the 10 % trimmed mean of the read depth, in 10 bp bins, across all 3 kb regions centred on selected TSSs. We focused our analysis on TSSs in non-coding regions to avoid confounding signals from overlapping mRNA transcripts.

#### *Identification of transcription start sites by cappable-seq*

To map TSSs globally we used cappable-seq. Duplicate cultures of *B. subtilis* strain 168 ca were grown until mid-exponential phase in LB media with shaking at 37 °C. Cells were harvested and flash frozen in liquid nitrogen. Total RNA was isolated as described previously with the exception that RNA concentration and quality was determined on an Agilent 2200 Tapestation following the manufacturer's instructions<sup>54</sup>. Library preparation and sequencing was done by Vertis Biotechnologie AG according to the protocol described by Ettwiller *et al.*<sup>22</sup>. Briefly, 5' triphosphorylated RNA was capped with 3'-desthiobiotin-TEG-guanosine 5' triphosphate (DTBGTP) using Vaccinia capping enzyme (New England Biolabs). Biotinylated RNA was captured and eluted from streptavidin beads to obtain 5' fragments of primary transcripts. These transcripts were poly(A) tailed with poly(A) polymerase before conversion of the 5' CAP moiety to a 5' monophosphate using CAP-clip Acid pyrophosphatase (Cellscript). An RNA adapter was ligated to the 5' monophosphate and cDNA synthesis was done with an oligo(dT)-adapter primer and M-MLV reverse transcriptase. cDNAs were amplified by PCR to a final concentration of 10-20 ng  $\mu\text{l}^{-1}$ . Full length cDNAs were fragmented and immobilised with streptavidin magnetic beads for blunting and ligation of the 3' Illumina sequencing adapter. The immobilised cDNA fragments were amplified via PCR. The sample libraries were mixed in equimolar amounts 200-500 bp fragments were purified from an agarose gel after electrophoresis. The libraries

were sequenced on an Illumina Nextseq 500 system with a read length of 75 bp. Individual sequence reads were mapped using Bowtie2<sup>51</sup>. The *B. subtilis* reference genome was that assigned Genbank accession numbers NC\_000964.3. Resulting Binary Alignment Map (BAM) files were used to generate wiggle plots using bam2wig.py<sup>52,53</sup>. For each strand of the chromosome, we assigned TSSs to base positions where the read depth increased more than 3-fold, compared to the previous base, in both experimental replicates.

#### *DNAse I footprinting*

DNA fragments were excised from pSR using *AatII* and *HindIII*. After end-labelling using  $\gamma^{32}$ -ATP and T4 PNK (NEB), footprints were done as previously described in buffer containing 40 mM Tris acetate pH 7.9, 50 mM KCl, 5 mM MgCl<sub>2</sub>, 500  $\mu$ M DTT and 12.5  $\mu$ g/ml Herring Sperm DNA<sup>47</sup>. Resulting DNA fragments were analysed on a 6 % denaturing gel. Subsequently, dried gels were exposed to a Biorad phosphorscreen that was scanned using a Biorad Personal Molecular Imager.

#### *Assignment of transcription start sites to horizontally acquired DNA*

To identify horizontally acquired genomic regions in different bacteria we used DarkHorse with genus level phylogenetic granularity<sup>55</sup>. Sections of DNA with high or low H-NS binding were identified using the ChIP-seq analysis of Kahramanoglou *et al*<sup>56</sup>.

#### **DATA AVAILABILITY**

The data that support these findings are available from the corresponding author on request. The *E. coli* RNA-seq, and *B. subtilis* cappable-seq, data are available in Array Express using accession numbers E-MTAB-9655 and E-MTAB-8582 respectively.

#### **FIGURE LEGENDS**

**Figure 1: Transcription start site pairs within horizontally acquired genes.** a)  $\beta$ -galactosidase activity derived from cryptic RNAP binding sites. Data are presented as mean values (n = 3 independent experiments) +/- SD and individual data points are overlaid as dot plots. b) Direction of transcription from cloned DNA fragments. c) Average forward or reverse  $\beta$ -galactosidase activity of all DNA fragments. d) Start sites mapped by primer extension for selected DNA fragments (orientations labelled a or b). Primer extension products in lanes 1 to 10, sizes in nucleotides (nt). Lanes 11-14 are sequencing reactions for calibration. e) Schematic representation of transcription start site pairs. Core promoter element sequences in the forward or reverse orientation are indicated by solid or open rectangles respectively. Speckled shading indicates converge of promoter elements on the same section of DNA. Transcription start sites shown as bent arrows. The positions of mutations (x) or deletions ( $\Delta$ ) are indicated. f) Effect of mutating shared core promoter elements. Data are presented as in panel a.

**Figure 2: Widespread divergent transcription from bidirectional promoter sequences in *Escherichia coli*.** a) Heatmaps made using global transcription start site (TSS) data<sup>19,22,23</sup> or position weight matrix analysis. TSSs on the top chromosome strand are aligned at the centre of the heatmap (bent arrow, labelled +1). Heatmap colour indicates abundance of bottom strand TSSs at that position.

The expansion shows the occurrence of bottom strand TSSs in a 50 bp window either side of all top strand promoters. b) Predominant DNA sequence motif associated with bidirectional or c) directional promoters. The x-axis break indicates the variable distance between -10 element and TSS at directional promoters. Each sequence motif was generated from 638 aligned promoters. d) a bidirectional promoter sequence between the *E. coli pfs* and *dgt* genes. TSSs are in uppercase. Promoter -10 elements are bold. Key sites of -10 element symmetry are underlined and correspond to the strongly conserved bases in panel b. The non-template strand bases at these positions, relative to the direction of transcription, are sequestered by  $\sigma^{70}$  to stabilise initial DNA unwinding<sup>5</sup>. e) Categorisation of bidirectional *E. coli* promoters according to nearby gene organisation. Percentages indicate the proportion of bidirectional promoters in each genomic context. For comparison, 89 % of the *E. coli* genome is coding whilst 6 %, 3 % and 2 % is intergenic DNA between co-directional, divergent and convergent genes respectively.

**Figure 3: Reciprocal stimulation between divergent transcription start sites.** a) Structure of RNAP bound to DNA (PDB: 6CA0)<sup>57</sup>. Relevant features labelled. b) DNA templates used for *in vitro* transcription. Sequences of promoter -10 elements (labelled) and TSSs (bent arrows) are shown. Plasmid vector DNA is shown by black lines and opposing DNA strands of the cloned bidirectional promoter sequence are shown by teal or grey lines. Interaction of  $\sigma^{70}$  R451 and the DNA backbone is indicated by dashes. Note that only transcription towards the *loop* terminator produces an RNA of defined length, detectable as a discrete band, following electrophoresis. Hence, to detect transcription in the opposite direction, it was necessary to invert the orientation of the cloned DNA sequence. c) Products of *in vitro* transcription (using templates in panel b) using either  $\sigma^{70}$  or the R451A derivative. The RNAI transcript is derived from the replication origin of the plasmid DNA template. The transcript of interest/RNAI signal intensity is 0.16, 0.05, 0.56, 0.11, 0.12, 0.06, 0.17, 0.09, 0.06, 0.05, 0.15, 0.06, 1.24 and 1.30 for lanes 1 to 14 respectively. The control promoter has the sequence 5'-TTGGCATATGAAATTTTGAGGATTATACTACACTTA-3'. A representative example of two separate experiments is shown. d,e) Aggregate profiles of transcription detected by genome-wide RNA-seq experiments. Each plot illustrates averaged sequence read depth across all 3 kb regions centred on bidirectional promoter sequences in non-coding DNA. Shaded areas of plots indicate signals above the background level f) A 17.5 kb section of the *E. coli* genome aligned with cappable-seq and RNA-seq reads mapping to the top (teal) or bottom (grey) DNA strands. Genes are denoted by red block arrows. Transcription start sites (TSSs) are denoted by gridlines and bent back arrows. Double arrow heads indicate divergent TSS pairs at bidirectional promoter sequences.

**Figure 4: Bidirectional promoter sequences are widespread in prokaryotes.** a,b) Heatmaps indicate abundance and position of TSSs on the bottom DNA strand, relative to the nearest top strand promoter (bent arrow). Species and phylogenetic relationships are indicated to left of heatmaps. c) DNA sequence motifs derived from divergent TSSs in *T. kodakarensis*.

**Figure 5: Coordinated regulation of divergent transcription units from bidirectional promoter sequences.** a) Organisation of the region between VC1303 and VC1304 in *Vibrio cholerae*. Transcription start sites are shown by bent arrows (+1) and the region footprinted by VpsT is underlined. The bidirectional promoter -10 region is bold with key positions of symmetry underlined. Position numbers indicate distances from the downstream end of the cloned DNA fragment subsequently used. b) Pattern of DNase I digestion with or without VpsT (2, 3, 4 or 5  $\mu$ M) and cyclic-di-GMP (50  $\mu$ M). The gel is calibrated with a Maxam-Gilbert GA ladder. The region protected by VpsT marked by a blue bar (triangles indicate VpsT induced DNase I hypersensitivity). A representative example of three experiments is shown. c) Transcripts generated from the VC1303-VC1304 intergenic region by RNA polymerase *in vitro* with or without 2  $\mu$ M VpsT and 50  $\mu$ M cyclic-di-GMP. The transcript of interest/RNAI signal intensity is 0.11, 0.02, 0.18 and 0.05 for lanes 1 to 4 respectively. A representative example of two separate experiments is shown. d)  $\beta$ -galactosidase activity derived from the VC1303-VC1304 intergenic region cloned in either orientation upstream of *lacZ*. Cells were supplied with VpsT



from plasmid pAMNF. Empty plasmid was used as a control. Bars are mean values (n = 3 independent experiments) +/- SD with individual data points overlaid as dot plots. *P* was derived from a two-sided paired student's *t*-test e) DNA templates to assess competition between RNA polymerase molecules during transcription *in vitro*. Promoter -10 and -35 elements are shown by black rectangles. TSSs are indicated by bent arrows. Plasmid vector DNA shown as black lines and opposing DNA strands of cloned bidirectional promoter sequences as teal or grey lines. f) Products of *in vitro* transcription using templates in panel e. The RNAI transcript is derived from the replication origin of the plasmid DNA template. The 134 nt RNA/129 nt RNA signal intensity is 0.68, not detectable, 0.09, 0.09, 4.48, 5.96, 0.39 and 0.32 in lanes 1 to 8 respectively. A representative example of two separate experiments is shown.

**Figure 6: Promoter bidirectionality has a different basis in prokaryotes and eukaryotes.**

## REFERENCES

1. Mejía-Almonte, C. *et al.* Redefining fundamental concepts of transcription initiation in bacteria. *Nat. Rev. Genet.* (2020) doi:10.1038/s41576-020-0254-8.
2. Browning, D. F. & Busby, S. J. W. The regulation of bacterial transcription initiation. *Nat. Rev. Microbiol.* **2**, 57–65 (2004).
3. Haberle, V. & Stark, A. Eukaryotic core promoters and the functional basis of transcription initiation. *Nat. Rev. Mol. Cell Biol.* **19**, 621–637 (2018).
4. Bae, B., Feklistov, A., Lass-Napiorkowska, A., Landick, R. & Darst, S. A. Structure of a bacterial RNA polymerase holoenzyme open promoter complex. *Elife* **4**, (2015).
5. Feklistov, A. & Darst, S. A. Structural basis for promoter -10 element recognition by the bacterial RNA polymerase  $\sigma$  subunit. *Cell* **147**, 1257–1269 (2011).
6. Kramm, K., Engel, C. & Grohmann, D. Transcription initiation factor TBP: old friend new questions. *Biochem. Soc. Trans.* **47**, 411–423 (2019).
7. Butler, J. E. F. The RNA polymerase II core promoter: a key component in the regulation of gene expression. *Genes Dev.* **16**, 2583–2592 (2002).
8. Core, L. J., Waterfall, J. J. & Lis, J. T. Nascent RNA sequencing reveals widespread pausing and divergent initiation at human promoters. *Science* **322**, 1845–1848 (2008).
9. Seila, A. C. *et al.* Divergent transcription from active promoters. *Science* **322**, 1849–1851 (2008).
10. Preker, P. *et al.* RNA exosome depletion reveals transcription upstream of active human promoters. *Science* **322**, 1851–1854 (2008).
11. He, Y., Vogelstein, B., Velculescu, V. E., Papadopoulos, N. & Kinzler, K. W. The antisense transcriptomes of human cells. *Science* **322**, 1855–1857 (2008).
12. Neil, H. *et al.* Widespread bidirectional promoters are the major source of cryptic transcripts in yeast. *Nature* **457**, 1038–1042 (2009).
13. Scruggs, B. S. *et al.* Bidirectional Transcription Arises from Two Distinct Hubs of Transcription Factor Binding and Active Chromatin. *Mol. Cell* **58**, 1101–1112 (2015).
14. Rege, M. *et al.* Chromatin Dynamics and the RNA Exosome Function in Concert to Regulate Transcriptional Homeostasis. *Cell Rep.* **13**, 1610–1622 (2015).
15. Wu, X. & Sharp, P. A. X-Divergent transcription: A driving force for new gene origination? *Cell* vol. 155 990 (2013).

- 492 16. Jin, Y., Eser, U., Struhl, K. & Churchman, L. S. The Ground State and Evolution of Promoter  
493 Region Directionality. *Cell* **170**, 889–898.e10 (2017).
- 494 17. Remus T. Dame, F.-Z. M. R. and D. C. G. Chromosome organization in bacteria: mechanistic  
495 insights into genome structure and function. *Nat. Rev. Genet.* (2019).
- 496 18. Browning, D. F. & Busby, S. J. W. Local and global regulation of transcription initiation in  
497 bacteria. *Nat. Rev. Microbiol.* **14**, 638–650 (2016).
- 498 19. Singh, S. S. *et al.* Widespread suppression of intragenic transcription initiation by H-NS.  
499 *Genes Dev.* **28**, 214–219 (2014).
- 500 20. Mitra, P., Ghosh, G., Hafeezunnisa, M. & Sen, R. Rho Protein: Roles and Mechanisms. *Annu.*  
501 *Rev. Microbiol.* **71**, 687–709 (2017).
- 502 21. Keseler, I. M. *et al.* The EcoCyc database: reflecting new knowledge about *Escherichia coli*  
503 K-12. *Nucleic Acids Res.* **45**, D543–D550 (2017).
- 504 22. Ettwiller, L., Buswell, J., Yigit, E. & Schildkraut, I. A novel enrichment strategy reveals  
505 unprecedented number of novel transcription start sites at single base resolution in a model  
506 prokaryote and the gut microbiome. *BMC Genomics* **17**, 199 (2016).
- 507 23. Thomason, M. K. *et al.* Global transcriptional start site mapping using differential RNA  
508 sequencing reveals novel antisense RNAs in *Escherichia coli*. *J. Bacteriol.* **197**, 18–28 (2015).
- 509 24. Singh, S. S., Typas, A., Hengge, R. & Grainger, D. C. *Escherichia coli*  $\sigma$  70 senses sequence  
510 and conformation of the promoter spacer region. *Nucleic Acids Res.* **39**, 5109–5118 (2011).
- 511 25. Warman, E., Forrest, D., Wade, J. T. & Grainger, D. C. Widespread divergent transcription  
512 from prokaryotic promoters. *bioRxiv* **44**, 2020.01.31.928960 (2020).
- 513 26. Santos-Zavaleta, A. *et al.* A unified resource for transcriptional regulation in *Escherichia coli*  
514 K-12 incorporating high-throughput-generated binding data into RegulonDB version 10.0.  
515 *BMC Biol.* **16**, (2018).
- 516 27. Mendoza-Vargas, A. *et al.* Genome-Wide Identification of Transcription Start Sites, Promoters  
517 and Transcription Factor Binding Sites in *E. coli*. *PLoS One* **4**, e7526 (2009).
- 518 28. Gill, E. E. *et al.* High-throughput detection of RNA processing in bacteria. *BMC Genomics* **19**,  
519 223 (2018).
- 520 29. Papenfort, K., Förstner, K. U., Cong, J. P., Sharma, C. M. & Bassler, B. L. Differential RNA-  
521 seq of *Vibrio cholerae* identifies the VqmR small RNA as a regulator of biofilm formation.  
522 *Proc. Natl. Acad. Sci. U. S. A.* **112**, E766–E775 (2015).
- 523 30. Kröger, C. *et al.* The primary transcriptome, small RNAs and regulation of antimicrobial  
524 resistance in *Acinetobacter baumannii* ATCC 17978. *Nucleic Acids Res.* **46**, 9684–9698  
525 (2018).
- 526 31. Sharma, C. M. *et al.* The primary transcriptome of the major human pathogen *Helicobacter*  
527 *pylori*. *Nature* **464**, 250–255 (2010).
- 528 32. Cortes, T. *et al.* Genome-wide Mapping of Transcriptional Start Sites Defines an Extensive  
529 Leaderless Transcriptome in *Mycobacterium tuberculosis*. *Cell Rep.* **5**, 1121–1131 (2013).
- 530 33. Jeong, Y. *et al.* The dynamic transcriptional and translational landscape of the model antibiotic  
531 producer *Streptomyces coelicolor* A3(2). *Nat. Commun.* **7**, 11605 (2016).
- 532 34. Fan, B. *et al.* dRNA-Seq Reveals Genomewide TSSs and Noncoding RNAs of Plant Beneficial  
533 *Rhizobacterium Bacillus amyloliquefaciens* FZB42. *PLoS One* **10**, e0142002 (2015).
- 534 35. Decker, K. B. & Hinton, D. M. Transcription regulation at the core: similarities among

535 bacterial, archaeal, and eukaryotic RNA polymerases. *Annu. Rev. Microbiol.* **67**, 113–39  
536 (2013).

537 36. Grünberger, F. *et al.* Next Generation DNA-Seq and Differential RNA-Seq Allow Re-  
538 annotation of the *Pyrococcus furiosus* DSM 3638 Genome and Provide Insights Into Archaeal  
539 Antisense Transcription. *Front. Microbiol.* **10**, 1603 (2019).

540 37. Babski, J. *et al.* Genome-wide identification of transcriptional start sites in the haloarchaeon  
541 *Haloferax volcanii* based on differential RNA-Seq (dRNA-Seq). *BMC Genomics* **17**, 629  
542 (2016).

543 38. Jäger, D., Förstner, K. U., Sharma, C. M., Santangelo, T. J. & Reeve, J. N. Primary  
544 transcriptome map of the hyperthermophilic archaeon *Thermococcus kodakarensis*. *BMC*  
545 *Genomics* **15**, 684 (2014).

546 39. Lamberte, L. E. *et al.* Horizontally acquired AT-rich genes in *Escherichia coli* cause toxicity  
547 by sequestering RNA polymerase. *Nat. Microbiol.* **2**, 16249 (2017).

548 40. Chen, J. *et al.* Stepwise Promoter Melting by Bacterial RNA Polymerase. *Mol. Cell* **78**, 275-  
549 288.e6 (2020).

550 41. Warman, E. A., Singh, S. S., Gubieda, A. G. & Grainger, D. C. A non-canonical promoter  
551 element drives spurious transcription of horizontally acquired bacterial genes. *Nucleic Acids*  
552 *Res.* **48**, 4891–4901 (2020).

553 42. Miller, J. Experiments in Molecular Genetics. (1972).

554 43. Haycocks, J. R. J. & Grainger, D. C. Unusually situated binding sites for bacterial transcription  
555 factors can have hidden functionality. *PLoS One* **11**, (2016).

556 44. Dugar, G. *et al.* High-Resolution Transcriptome Maps Reveal Strain-Specific Regulatory  
557 Features of Multiple *Campylobacter jejuni* Isolates. *PLoS Genet.* **9**, e1003495 (2013).

558 45. Singh, N. & Wade, J. T. Identification of regulatory RNA in bacterial genomes by genome-  
559 scale mapping of transcription start sites. *Methods Mol. Biol.* **1103**, 1–10 (2014).

560 46. Crooks, G. E., Hon, G., Chandonia, J.-M. & Brenner, S. E. WebLogo: A Sequence Logo  
561 Generator. doi:10.1101/gr.849004.

562 47. Haycocks, J. R. J. *et al.* The quorum sensing transcription factor AphA directly regulates  
563 natural competence in *Vibrio cholerae*. *PLoS Genet.* **15**, e1008362 (2019).

564 48. Kolb, A., Kotlarz, D., Kusano, S. & Ishihama, A. Selectivity of the *Escherichia coli* RNA  
565 polymerase Eσ38 for overlapping promoters and ability to support CRP activation. *Nucleic*  
566 *Acids Res.* **23**, 819–826 (1995).

567 49. Savery, N. J. *et al.* Transcription activation at class II CRP-dependent promoters: Identification  
568 of determinants in the C-terminal domain of the RNA polymerase α subunit. *EMBO J.* **17**,  
569 3439–3447 (1998).

570 50. Stead, M. B. *et al.* RNAsnap<sup>TM</sup>: A rapid, quantitative and inexpensive, method for isolating  
571 total RNA from bacteria. *Nucleic Acids Res.* **40**, e156 (2012).

572 51. Langmead, B. & Salzberg, S. L. Fast gapped-read alignment with Bowtie 2. *Nat. Methods* **9**,  
573 357–359 (2012).

574 52. Afgan, E. *et al.* The Galaxy platform for accessible, reproducible and collaborative biomedical  
575 analyses: 2018 update. *Nucleic Acids Res.* **46**, W537–W544 (2018).

576 53. Wang, L., Wang, S. & Li, W. RSeQC: quality control of RNA-seq experiments.  
577 *Bioinformatics* **28**, 2184–2185 (2012).

- 578 54. Forrest, D., James, K., Yuzenkova, Y. & Zenkin, N. Single-peptide DNA-dependent RNA  
579 polymerase homologous to multi-subunit RNA polymerase. *Nat. Commun.* **8**, 15774 (2017).
- 580 55. Podell, S., Gaasterland, T. & Allen, E. E. A database of phylogenetically atypical genes in  
581 archaeal and bacterial genomes, identified using the DarkHorse algorithm. *BMC*  
582 *Bioinformatics* **9**, 419 (2008).
- 583 56. Kahramanoglou, C. *et al.* Direct and indirect effects of H-NS and Fis on global gene  
584 expression control in *Escherichia coli*. *Nucleic Acids Res.* **39**, 2073–2091 (2011).
- 585 57. Narayanan, A. *et al.* Cryo-EM structure of *Escherichia coli*  $\sigma$  70 RNA polymerase and  
586 promoter DNA complex revealed a role of  $\sigma$  non-conserved region during the open complex  
587 formation. *J. Biol. Chem.* **293**, 7367–7375 (2018).

## ACKNOWLEDGEMENTS

**FUNDING:** This work was funded by a Leverhulme Trust project grant (RPG-2018-198) and Wellcome Trust Investigator Award (212193/Z/18/Z) to DCG. **AUTHOR CONTRIBUTIONS:** The work was conceived and supervised by D.C.G. The *B. subtilis* TSS mapping and, *in vitro* analysis of different TSS spacings, was done by D.F. Analysis of the *V. cholerae* VC1303-VC1304 regulatory region was done by T.G. and J.R.J.H. All other experimental work was done by E.A.W. Computational analysis was done by D.C.G., J.T.W. and D.F. All authors contributed to data analysis and interpretation. The manuscript was written by D.C.G. with input from all authors.

## COMPETING INTERESTS STATEMENT

The authors declare that there are no competing interests.

Figure 1

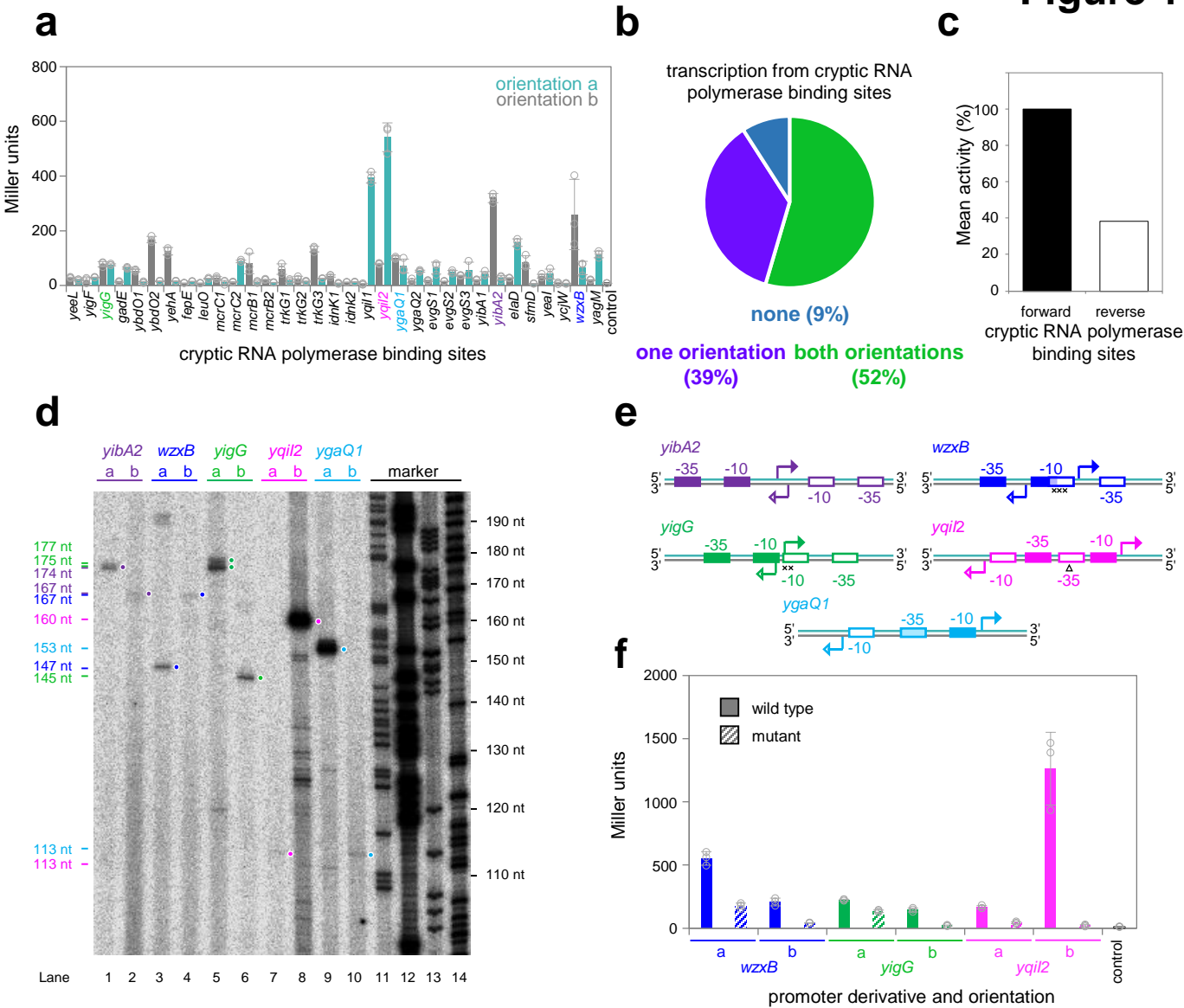


Figure 2

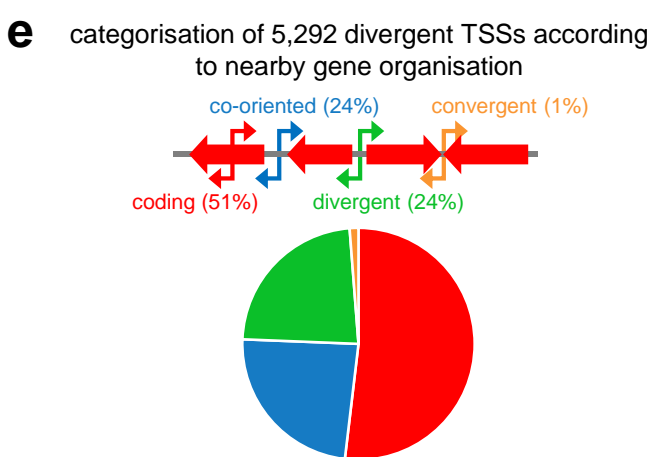
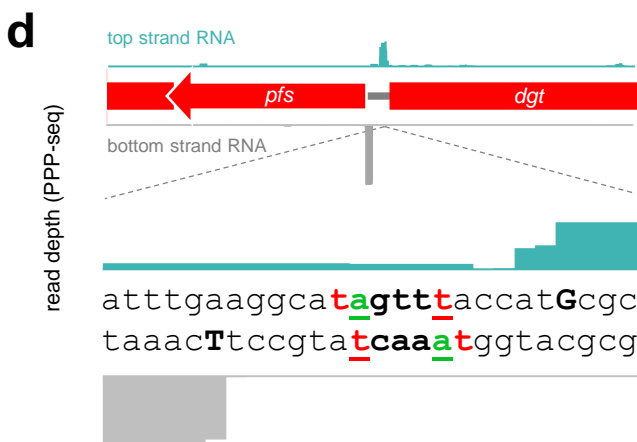
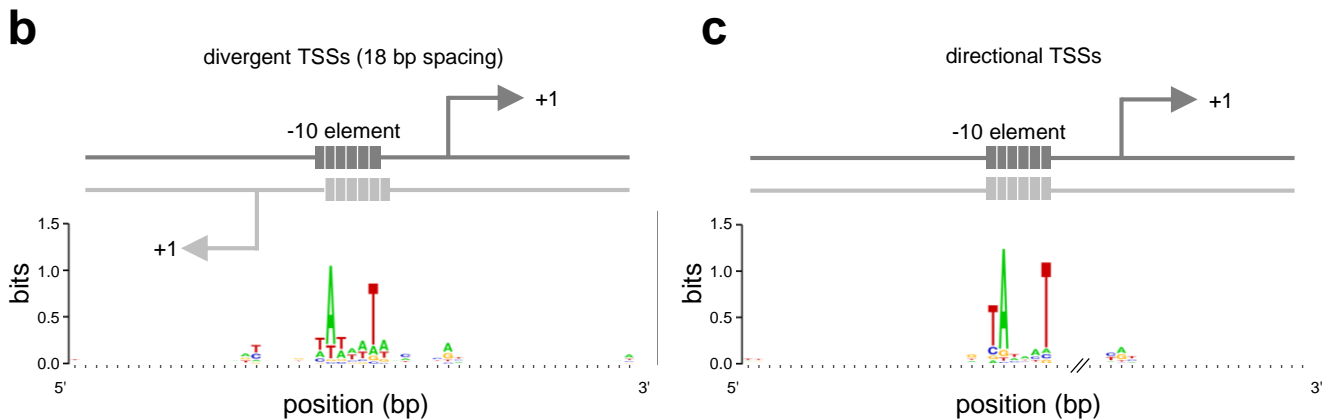
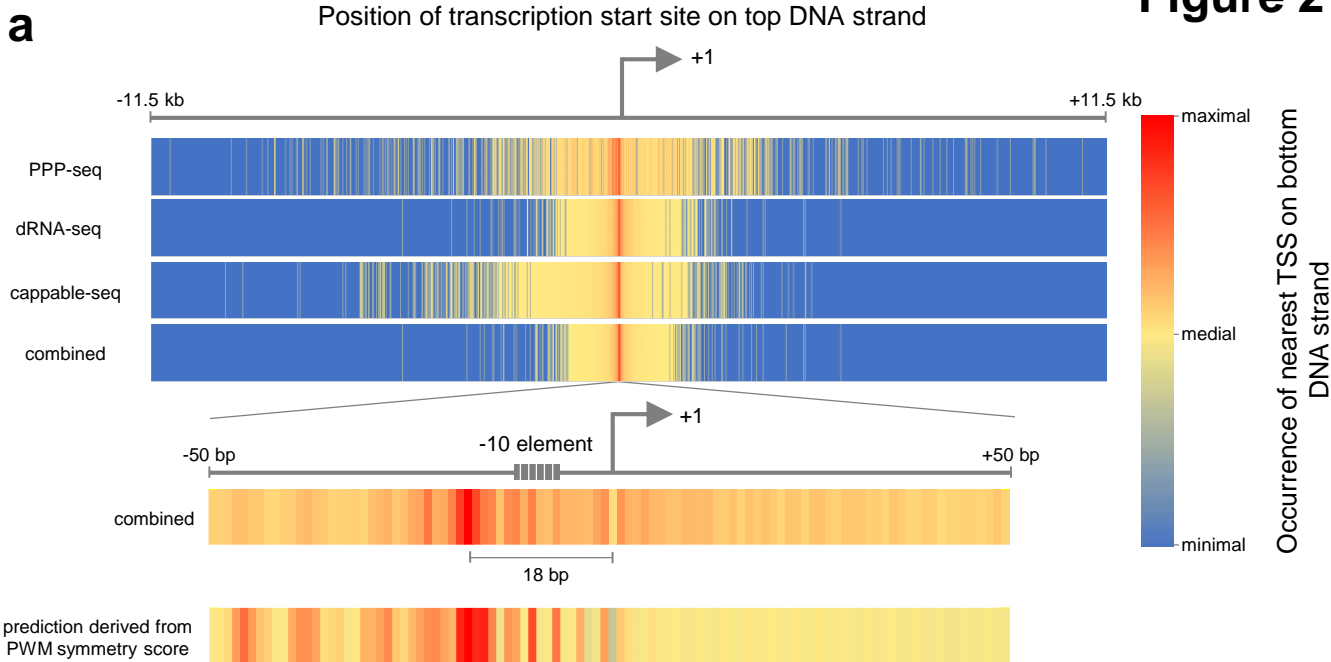


Figure 3

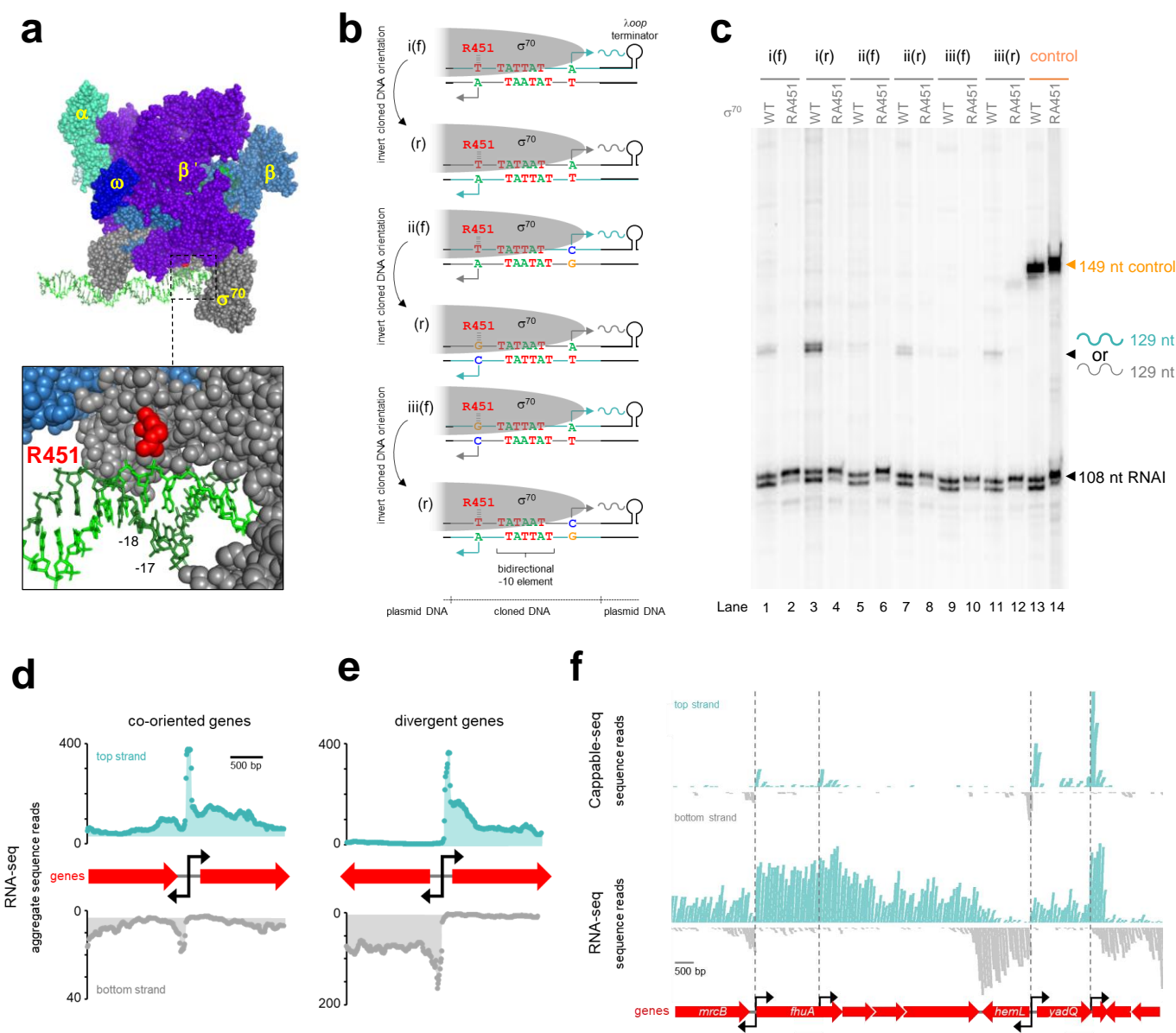


Figure 4

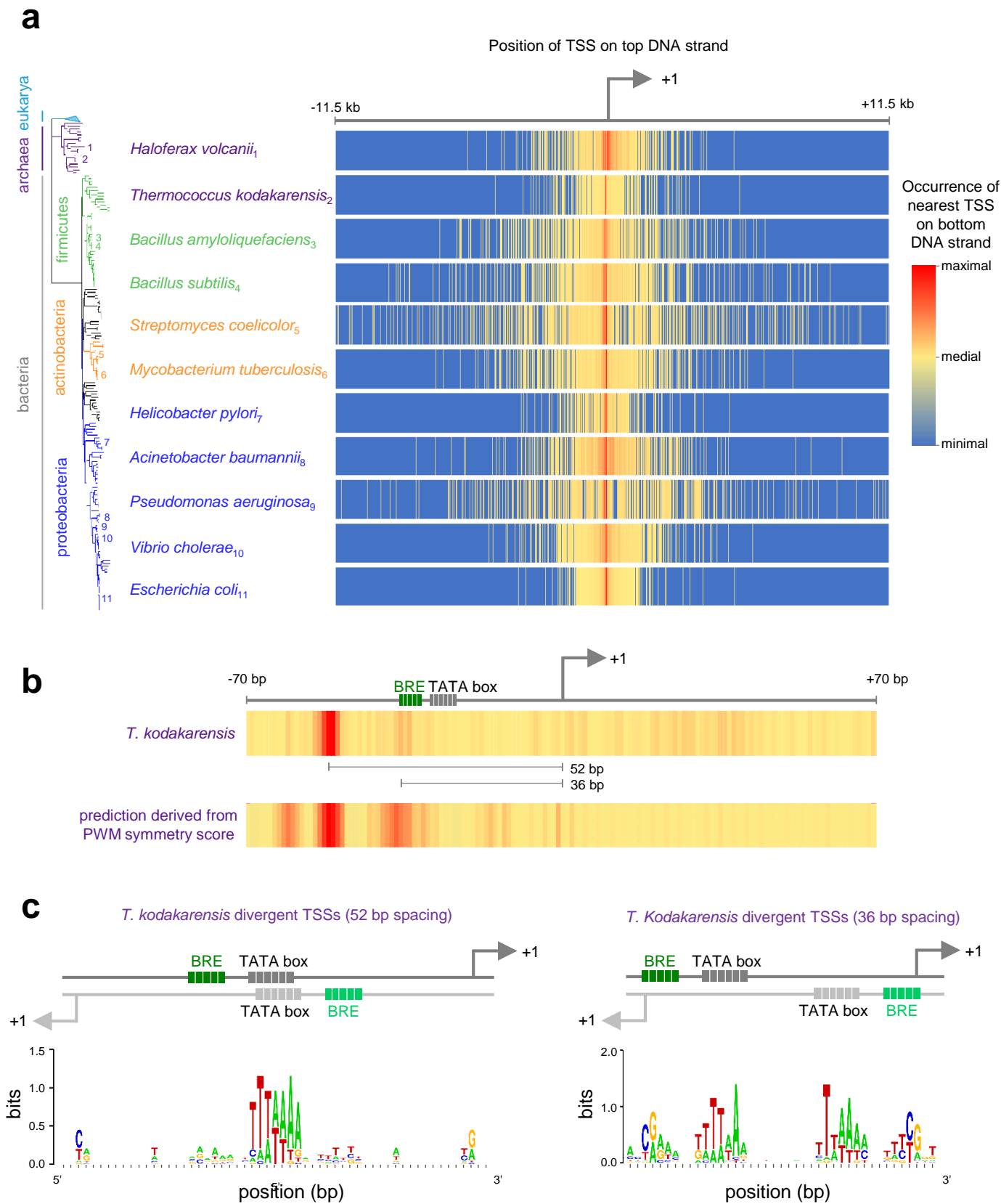




Figure 5

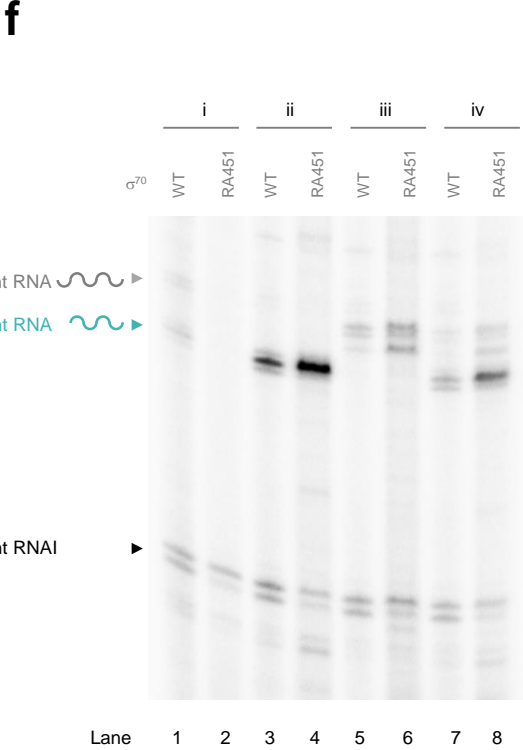
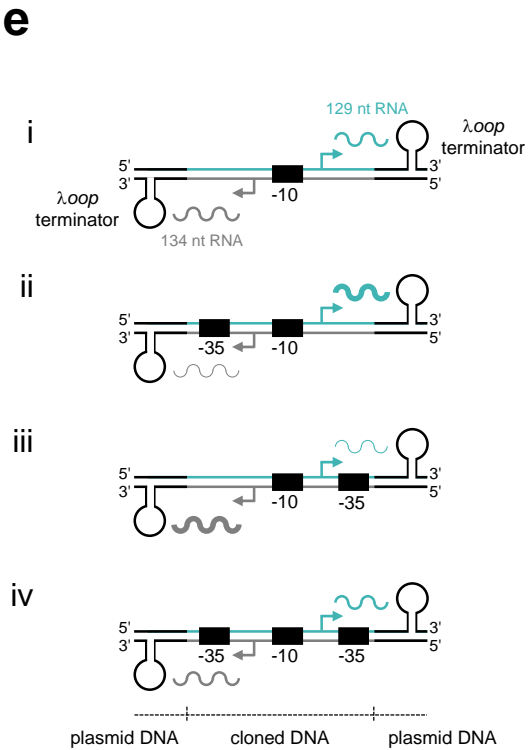
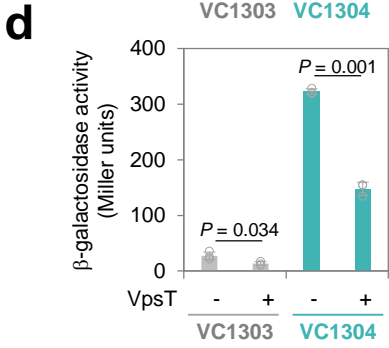
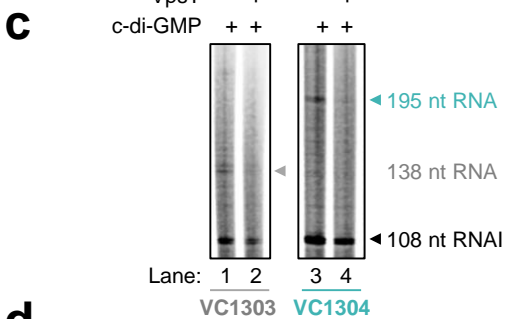
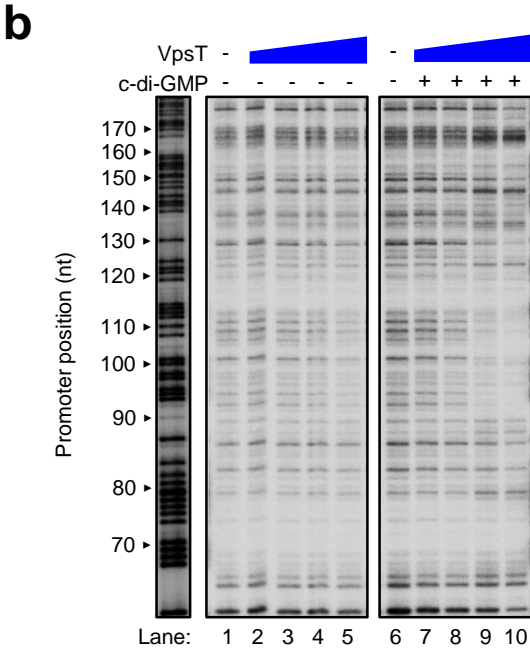
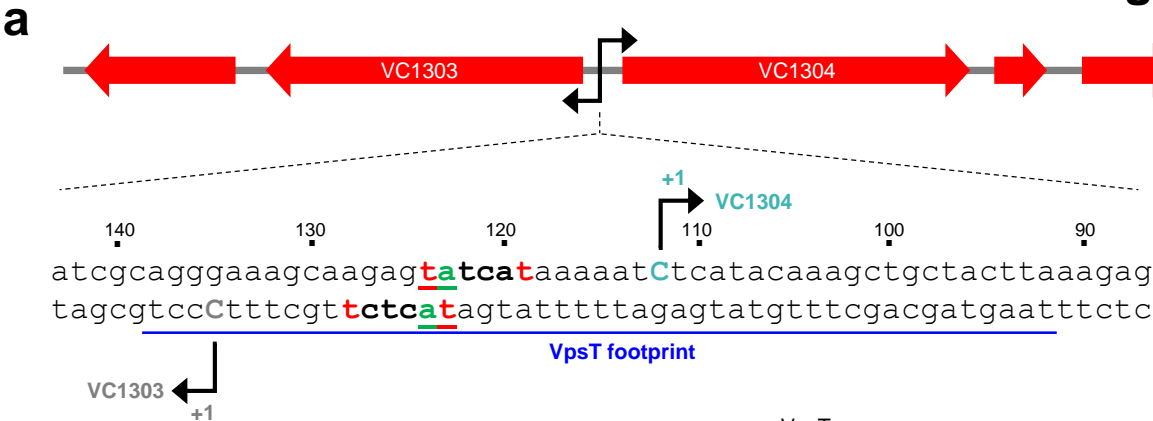


Figure 6

